ISSN 1343-2230
CNS-REP-31
ISSN 1346-244X
RIKEN-AF-NP-397
RUP-01-3
April, 2001

CNS

CNS Report

Isobaric analog state of ^{14}Be

S. Takeuchi, S. Shimoura, T. Motobayashi, H. Akiyoshi,
Y. Ando, N. Aoi, Zs. Fülöp, T. Gomi, Y. Higurashi,
M. Hirai, N. Iwasa, H. Iwasaki, Y. Iwata, H. Kobayashi,
M. Kurokawa, Z. Liu, T. Minemura, S. Ozawa,
H. Sakurai, M. Serata, T. Teranishi, K. Yamada,
Y. Yanagisawa and M. Ishihara

submitted to Physics Letters B

Center for Nuclear Study (CNS)

Graduate School of Science, the University of Tokyo
Wako Branch at RIKEN, Hirosawa 2-1, Saitama 351-0198, Japan
Correspondence: cnsoffice@cns.s.u-tokyo.ac.jp

Isobaric analog state of ^{14}Be

S. Takeuchi [a,*], S. Shimoura [b], T. Motobayashi [a], H. Akiyoshi [c], Y. Ando [a], N. Aoi [d], Zs. Fülöp [e], T. Gomi [a], Y. Higurashi [a], M. Hirai [f], N. Iwasa [g], H. Iwasaki [b], Y. Iwata [f], H. Kobayashi [a], M. Kurokawa [b], Z. Liu [h], T. Minemura [c], S. Ozawa [c], H. Sakurai [d], M. Serata [a], T. Teranishi [b], K. Yamada [a], Y. Yanagisawa [c] and M. Ishihara [c]

[a] *Department of Physics, Rikkyo University, Toshima, Tokyo 171-8501, Japan*

[b] *Center for Nuclear Study (CNS), University of Tokyo, Wako, Saitama 351-0198, Japan*

[c] *The Institute of Physical and Chemical Research (RIKEN), Wako, Saitama 351-0198, Japan*

[d] *Department of Physics, University of Tokyo, Bunkyo, Tokyo 113-0033, Japan*

[e] *Institute of Nuclear Research of the Hungarian Academy of Sciences, 4001 Debrecen, P.O.Box 51, Hungary*

[f] *National Institute of Radiological Sciences, Inage, Chiba 263-8555, Japan*

[g] *Department of Physics, Tohoku University, Aoba, Sendai, Miyagi 980-8578, Japan*

[h] *Institute of Modern Physics, Chinese Academy of Sciences, Lanzhou, 730000, China*

Abstract

The Isobaric Analog State (IAS) of the neutron-dripline nucleus ^{14}Be has been found for the first time in a charge-exchange reaction ^{14}Be(p,n)^{14}B* in inverse kinematics at $E(^{14}\mathrm{Be}) = 74\ A$ MeV. The excitation energy and width of the observed IAS were measured to be 17.06 ± 0.03 MeV and 0.11 ± 0.05 MeV (FWHM), respectively. The Coulomb displacement energy and the measured width of the IAS are discussed in connection with a possible neutron-halo structure of the ^{14}Be nucleus.

Key words: Isobaric analog state, Charge-exchange reactions, Radioactive beam experiment, Coulomb displacement energy, Halo structure
PACS: 25.40.Kv, 25.45.Kk, 25.60.Lg, 27.20.+n

Preprint submitted to Physics Letters B

The halo structure of the neutron-dripline nucleus ^{14}Be has been investigated by various approaches [1–4]. A large root-mean-square (rms) radius was obtained from interaction cross section measurements [1, 2]. This large radius can be attributed to a contribution of $(2s_{1/2})^2$ component in the wave function of the valence neutrons assuming a core+2n structure in ^{14}Be [2]. This view is supported by a recent kinematically complete measurement of a dissociation reaction [3]. It suggested that the halo wave function contains a large $(2s_{1/2})^2$ admixture. The halo structure of ^{14}Be was also revealed in a narrow momentum distribution of ^{12}Be observed in the ^{14}Be fragmentation [4]. Another aspect of the halo structure of ^{14}Be may be explored by studying its Isobaric Analog State (IAS). Since the wave function of the IAS is essentially the same as that of its isobaric partner, possible exotic natures of ^{14}Be may be traced in properties of the IAS such as the Coulomb displacement energy (ΔE_C) and the width of the IAS.

Recently the charge-exchange reaction ^{11}Li(p,n)^{11}Be* was measured by Teranishi *et al.* [5] to study the IAS of ^{11}Li in ^{11}Be. They observed the IAS and determined its energy and width. The extracted ΔE_C and decay mode could be related to the halo structure of ^{11}Li [5, 6]. In the present study, we applied this method to the neutron-dripline nucleus ^{14}Be. The IAS of ^{14}Be in ^{14}B was excited by the charge-exchange reaction ^{14}Be(p,n)^{14}B*. The deduced quantities are the excitation energy and width of the IAS. The angular distribution of the ^{14}Be(p,n)^{14}B*(IAS) reaction was also measured. The ΔE_C is extracted from the excitation energy of the IAS in comparison with the energy of its isospin partner ^{14}Be. It gives information on the spatial extension of the wave function of the exchanged proton in the IAS. The observed width of the IAS gives a clue to the configuration of the valence neutrons in the ground state of ^{14}Be.

We have measured the ^{14}Be(p,n)^{14}B* reaction in inverse kinematics using a ^{14}Be radioactive beam at 74 A MeV. The energy-systematics among the neighboring isospin partners suggests that the IAS in ^{14}B locates above many particle-decay thresholds (see Fig. 1). In the inverse kinematics, decay particles from the unbound ^{14}B state are emitted in the forward direction with beam velocities, allowing efficient detection of these particles. The excitation energy of ^{14}B* was reconstructed from the momentum vectors of all the decay particles measured in coincidence.

The IAS of ^{14}Be is characterized by its isospin of $T = 3$ and decays only into the ^{12}Be+p+n channel ($T = 3$ or 2). Because of the isospin selectivity, other decay channels with $T = 2$ are forbidden (see Fig. 1). Therefore, the IAS is found only in the decay energy spectrum of the ^{12}Be+p+n system.

* Corresponding author.
Email address: takeuchi@ne.rikkyo.ac.jp (S. Takeuchi).

The (p,n) reaction populates both the Fermi ($\Delta S = 0$, $\Delta L = 0$ and $T_f = T_i$) and Gamow-Teller ($\Delta S = 1$, $\Delta L = 0$ and $T_f = T_i, T_i \pm 1$) states. To distinguish between them, we performed an additional measurement of the ^{14}Be(d,2n) reaction where Fermi transitions are suppressed [9]. Another indication for the Fermi transition is in the angular distribution of the (p,n) reaction. Because of its zero angular-momentum transfer, the distribution is expected to exhibit forward peaking. As a whole, the IAS can be identified by comparing the decay energy spectra obtained with a hydrogen and a deuterium targets, and by analyzing the angular distribution of the center-of-mass of the ^{12}Be+p+n system, *i.e.* ^{14}B*.

The experiment was performed at the RIKEN Accelerator Research Facility. A secondary beam of ^{14}Be was produced by using the projectile fragmentation of a 100 A MeV ^{18}O beam on a 1110 mg/cm^2 thick ^{9}Be target, and selected by the RIKEN Projectile Fragment Separator (RIPS) [10]. Energy of the incident ^{14}Be beam was determined event-by-event by measuring the time-of-flight (TOF) over the 5.3 m flight path between 0.5 mm and 0.3 mm thick plastic scintillators mounted in the beam line, and was 74 $\pm$ 4 A MeV in the middle of a secondary target. The secondary beam was identified by a ΔE - TOF method, where a major impurity was ^{11}Li. A typical intensity of the ^{14}Be beam was 10^4 cps, and a purity was around 80%. After traversing through the plastic-scintillator detectors, the ^{14}Be beam was focused on a $(CH_2)_n$, $(CD_2)_n$ or C target with the thicknesses of 187, 204 and 152 mg/cm^2, respectively. The C target was used to subtract the contributions from carbon nuclei in the $(CH_2)_n$ and $(CD_2)_n$ targets.

The decay particles from ^{14}B* were detected in coincidence by a plastic scintillator hodoscope with a 1 $\times$ 1 m^2 active area, which was located at 4.9 m downstream from the target with its symmetry axis along the beam line. In order to minimize the energy losses and the multiple scattering for charged particles in the flight path, the hodoscope was installed in a vacuum chamber [11]. The hodoscope consisted of a 5-mm thick ΔE plane and two 60-mm thick E planes ($E1$, $E2$). The ΔE plane was divided horizontally into 13 slats, and the $E1$ and $E2$ planes consisted of 16 and 13 scintillator bars set perpendicular to the ΔE slats, respectively. The hodoscope was thus divided into 13 $\times$ 16 (or 13 for $E2$) segments. The widths of the scintillator slats and bars were taken to be narrower in the central part (40 mm for the ΔE plane and 38 mm for the $E1$ plane) to improve the balance of the counting rate among the scintillator bars; the widths of the other ΔE and E scintillator bars were 100 mm and 75 mm, respectively. Information on the particle hit position was obtained by the segmentation and time difference between signals from two photomultipliers attached to both ends of each scintillator bar. Velocities of the decay particles were determined by the TOF over the 4.9 m flight path between the target and the hodoscope. Resolutions of TOF were about 1.2% (FWHM) for charged particles and about 1.5% (FWHM) for neutrons at the

energies of 74 A MeV. Charged particles were identified by using the ΔE - TOF and E - TOF methods. For neutron detection, the ΔE plane served as a charged-particle veto. The momentum vectors of the decay particles were determined by combining their velocities and hit positions on the hodoscope.

The extracted momentum vectors ($\vec{p}_i$) are used to reconstruct the decay energy spectrum of the ^{12}Be+p+n system and the angular distribution of ^{14}B*. The decay energy is defined as the difference between the invariant mass and the threshold energy $\Sigma_i M_i$ (total rest mass of all the decay particles):

$$E_{\rm d} = M(^{14}{\rm B}^*) - \sum_i M_i, \tag{1}$$

where the invariant mass $M(^{14}$B$^*)$ is given by

$$M(^{14}{\rm B}^*) = \sqrt{\left(\sum_i E_i\right)^2 - \left|\sum_i \vec{p}_i\right|^2}. \tag{2}$$

The resolution of the decay energy $E_{\rm d}$ was estimated to be 0.15 MeV (FWHM) at $E_{\rm d} = 0.3$ MeV by a Monte Carlo simulation, which is roughly proportional to $\sqrt{E_{\rm d}}$. The simulation includes the beam size, effects of energy losses in the target and geometry of the hodoscope and time and position resolutions of the detectors. The detector acceptance is represented by the dotted curve in Fig. 2 (a), which was also estimated by a Monte Carlo simulation. In the calculation of the acceptance we assumed the sequential decay (^{14}B$^* \rightarrow {}^{13}$Be+p $\rightarrow {}^{12}$Be+p+n) with isotropic angular distributions in the center-of-mass system of ^{14}B*. Figures 2 (a) and (b) show the decay energy spectra of the ^{12}Be+p+n system for the (p,n) and (d,2n) reactions, respectively. Each spectrum was obtained by subtracting the contributions of the carbon nuclei in the $(CH_2)_n$ and $(CD_2)_n$ targets. The error bars involve only statistical uncertainties. The systematic error of absolute magnitude is evaluated to be about 10%, which is due to the uncertainties in the neutron detection efficiency and the reaction losses of the charged particles in the hodoscope.

As shown in Fig. 2, a prominent peak is observed at $E_{\rm d} \simeq 0.3$ MeV in the spectrum of the (p,n) reaction, whereas it is not apparent in that of the (d,2n) reaction. This feature is attributed to the $\Delta S = 0$ character of the peak, because both $\Delta S = 0$ and 1 transitions can occur in the (p,n) reaction while $\Delta S = 0$ is suppressed in the (d,2n) reaction.

The laboratory-frame angular distribution of ^{14}B* is shown in Fig. 3, where the distribution is corrected for the detector acceptance. It corresponds to the prominent peak in Fig. 2 (a). In a framework of PWBA, the differential cross section as a function of momentum transfer q is characterized by the spherical

Bessel function $j_\ell(qR)$, where ℓ and R denote transferred angular momentum (corresponding to ΔL) and nuclear radius, respectively. The radius R was assumed to be $1.62 \times 14^{1/3}$ fm as discussed later. The observed distribution was fitted with the spherical Bessel function folded with the experimental resolution. In Fig. 3, the solid, dashed and dotted curves show the results of the fitting with $j_0(qR)$, $j_1(qR)$ and $j_2(qR)$, respectively. As shown in Fig. 3, the best fit was obtained with $j_0(qR)$, indicating that the observed peak in the decay energy spectrum is characteristic of the $\Delta L = 0$ angular momentum transfer.

In order to confirm the isospin of the prominent peak in Fig. 2 (a), we have examined the decay energy spectrum in the ^{12}Be+d channel. This channel is relevant to $T = 2$ state of ^{14}B* instead of $T = 3$ for the IAS (see Fig. 1). In this spectrum no evident peak was seen at the energy corresponding to the prominent peak, suggesting the $T = 3$ nature of the peak observed in the ^{12}Be+p+n channel.

As discussed above, the peak observed in the (p,n) reaction at $E_{\rm d} \simeq 0.3$ MeV exhibits the characteristics of $\Delta S = 0$, $\Delta L = 0$, and $T_{\rm f} = T_{\rm i}$ $(= 3)$. Therefore the peak is assigned to the IAS of ^{14}Be$_{\rm g.s.}$. Note that the spin and parity of the observed IAS should be the same (0^+) as those of ground state in ^{14}Be. In order to deduce the resonance energy and natural width of the IAS, the peak was fitted with a Gaussian function and a background with a shape of a 3-body phase space (see Fig. 2 (c)). The $E_{\rm d}$ resolution, detector acceptance and angular distribution of ^{14}B* were taken into account in the fitting procedure. The energy and width of the peak were deduced to be 0.29 ± 0.02 MeV and 0.11 ± 0.05 MeV (FWHM), respectively. The errors contain the statistical one and the systematic uncertainty in the absolute magnitude of TOF.

Using the known threshold energy 16.77 MeV for the ^{12}Be+p+n channel [7], the excitation energy of the IAS was determined to be 17.06 ± 0.03 MeV with respect to the ground state of ^{14}B. The Coulomb displacement energy $(\Delta E_{\rm c})$ was obtained to be 1.62 ± 0.11 MeV for the pair of ^{14}Be and its IAS. This is smaller than the $\Delta E_{\rm C}$ values of 1.97 MeV for ^{10}Be and 1.83 MeV for ^{12}Be [12]. Figure 4 (a) shows experimental $\Delta E_{\rm C}$ values plotted as a function of neutron number (N). The $\Delta E_{\rm C}$ values for Li and Be isotopes depend similarly on N. A large decrease of $\Delta E_{\rm C}$ from ^{12}Be to ^{14}Be is observed and a similar decrease is seen in ^{9}Li to ^{11}Li. Since the small $\Delta E_{\rm C}$ of ^{11}Li could be related to the halo structure [5, 13], the small $\Delta E_{\rm C}$ of ^{14}Be may also be understood by the halo effect.

In order to relate the $\Delta E_{\rm C}$ to the nuclear radius, a liquid-drop model may be used. Assuming uniform charge distribution, the A-dependence of $\Delta E_{\rm C}$ is expressed [14] as

$$\Delta E_{\rm C} = E_{\rm C}(A, Z+1) - E_{\rm C}(A, Z), \tag{3}$$

where E_C is written as

$$E_C = \frac{3Z^2e^2}{5r_0A^{1/3}}\left[1 - 5\left(\frac{3}{16\pi Z}\right)^{2/3}\right]. \quad (4)$$

With a common radius parameter of $r_0 = 1.51$ fm, this expression provides ΔE_C values of 1.94, 1.83 and 1.74 MeV for Be isotopes of $A = 10$, 12 and 14, respectively. The dashed and dotted curves in Fig. 4 (a) show the predictions for Li and Be isotopes. Though the overall trend of the experimental data is reproduced by the prediction, the model overestimates for ^{14}Be and ^{11}Li. In order to explain the experimental value of ΔE_C for ^{14}Be, the magnitude of r_0 should be 1.62 ± 0.11 fm instead of 1.51 fm. This larger r_0 value suggests the halo structure of ^{14}Be. A large difference between ^{14}Be (^{11}Li) and other Be (Li) isotopes is also seen in the systematics of rms radii [1, 2] for Li and Be isotopes (see Fig. 4 (b)). Large radii are deduced for ^{11}Li and ^{14}Be by interaction cross section measurements. Using the present r_0 value, the rms radius is deduced to be 3.02 ± 0.21 fm for ^{14}Be. This is consistent with 3.10 ± 0.15 fm extracted from the interaction cross section [2].

The large radius of ^{14}Be may be interpreted as an effect of two loosely bound neutrons. By taking a model where ^{14}Be is decomposed into the core part (^{12}Be) and the valence nucleons (2N) [15], the ΔE_C for ^{14}Be may be given as

$$\Delta E_C(^{14}\mathrm{Be}) = \frac{4}{6}\Delta E_C(^{12}\mathrm{Be}) + \frac{2}{6}\Delta E_C(2\mathrm{N}). \quad (5)$$

Combining the experimental value of $\Delta E_C(^{14}$Be) with the known value of $\Delta E_C(^{12}\mathrm{Be}) = 1.83 \pm 0.05$ MeV, a value of 1.20 ± 0.34 MeV is deduced for $\Delta E_C(2\mathrm{N})$. Assuming that the valence proton in the IAS of ^{14}Be stays out of the core volume, $\Delta E_C(2\mathrm{N})$ may be approximated as $Z(=4)e^2\langle 1/r\rangle$, where r denotes the distance of the valence proton from the center of the core (^{12}Be). We obtained the value of $\langle 1/r\rangle^{-1} = 4.8 \pm 1.4$ fm. Estimations of the radius of the two loosely bound neutrons were made independently by Suzuki *et al.* [2] assuming a core+2n structure in ^{14}Be. They deduced the radius to be $r_{\mathrm{rms}}(\mathrm{n})$ $= 4.9 \pm 0.5$ fm and 5.6 ± 0.7 fm using an optical limit of the Glauber model and a few-body reaction model, respectively. The present value supports these large radii, which can be related to the halo structure of ^{14}Be.

In a recent plausible view, a mixture of $(2s_{1/2})^2$ and $(1d_{5/2})^2$ configurations is expected for the halo wave function [2, 3]. Since the particle-decay width can be affected by the spectroscopic factor and the angular momentum l of the valence nucleon, the observed width of the IAS may provide information of the valence proton configuration and hence the configuration of the neutrons in ^{14}Be. If the IAS is assumed to decay into the "^{13}Be-core" and the exchanged proton system, the exchanged proton decays with the orbital angular momentum $l =$

0 or 2. The particle-decay width for the angular momentum $l = 2$ is suppressed by comparison with the one for $l = 0$. For the present case, $\Gamma_0^0 = 0.24$ MeV and $\Gamma_2^0 = 0.001$ MeV are obtained from the expression proposed by Peräjärvi *et al.* [16] as,

$$\Gamma_l^0 = 2P_l \frac{3\hbar^2}{2\mu a^2}, \tag{6}$$

where P_l and μ denote the penetrability and the reduced mass and the channel radius a is assumed to be $1.62 \times 14^{1/3}$ fm. Therefore the width Γ_2^0 can be neglected as compared with Γ_0^0.

The observed width Γ may thus be given with the s-wave spectroscopic factor α by

$$\Gamma = \Gamma_0 + \Gamma_2 = \alpha\Gamma_0^0 + (1-\alpha)\Gamma_2^0 \simeq \alpha\Gamma_0^0. \tag{7}$$

The s-wave spectroscopic factor of 46 $\pm$ 21% is extracted from the observed width of $\Gamma = 0.11 \pm 0.05$ MeV. It supports the results of other studies [2, 3] which suggest a considerable contribution of the $2s_{1/2}$ orbital in the ^{14}Be ground state.

In summary, charge-exchange reaction ^{14}Be(p,n)^{14}B* has been measured in inverse kinematics at $E(^{14}\mathrm{Be}) = 74$ A MeV. The particle-unbound analog state (IAS) of ^{14}Be has been found in the decay energy spectrum of ^{12}Be+p+n system. The excitation energy and width of the IAS were measured to be 17.06 $\pm$ 0.03 MeV and 0.11 $\pm$ 0.05 MeV (FWHM), respectively. A relatively small Coulomb displacement energy of 1.62 $\pm$ 0.11 MeV was deduced between the ground state of ^{14}Be and its IAS, indicating the spatial extension of the wave function of the exchanged proton in the IAS. The observed large particle-decay width supports a large mixing of the $(2s_{1/2})^2$ configuration in the halo wave function. These results suggest a considerable contribution of the $2s_{1/2}$ orbital in the ground state of ^{14}Be.

We would like to thank the RIKEN Ring Cyclotron staff members for their operation during the experiment. The present study was partially supported by the Grant-In-Aid for Scientific Research of the Japan Ministry of Education, Science and Culture under the program numbers (B) 08454069. One of the authors, S.T., is grateful to the support of the RIKEN Junior Research Associate Program.

References

[1] I. Tanihata et al., Phys. Lett. B206 (1988) 592.
[2] T. Suzuki et al., Nucl. Phys. A658 (1999) 313.
[3] M. Labiche et al., Phys. Rev. Lett. 86 (2001) 600.
[4] M. Zahar et al., Phys. Rev. C48 (1993) R1484.
[5] T. Teranishi et al., Phys. Lett. B407 (1997) 110.
[6] S. Shimoura et al., Nucl. Phys. A630 (1997) 387c.
[7] G. Audi and A. H. Wapstra, Nucl. Phys. A595 (1995) 409.
[8] A. V. Belozyorov et al., Nucl. Phys. A636 (1998) 419.
[9] D. P. Stahel et al., Phys. Rev. C20 (1979) 1680.
[10] T. Kubo et al., Nucl. Inst. Meth. B70 (1992) 309.
[11] I. Hisanaga et al., RIKEN Accel. Prog. Rep. 31 (1998) 162.
[12] F. Azjenberg-Selove, Nucl. Phys. A490 (1988) 1.; A506 (1990) 1.
[13] T. Suzuki and T. Otsuka, Nucl. Phys. A635 (1998) 86.
[14] A. Bohr and B. R. Mottelson, Nuclear Structure Vol. 1 (Benjamin, New York, 1969) 145.
[15] Y. Suzuki and K. Yabana, Phys. Lett. B272 (1991) 173.
[16] K. Peräjärvi et al., Phys. Lett. B492 (2000) 1.

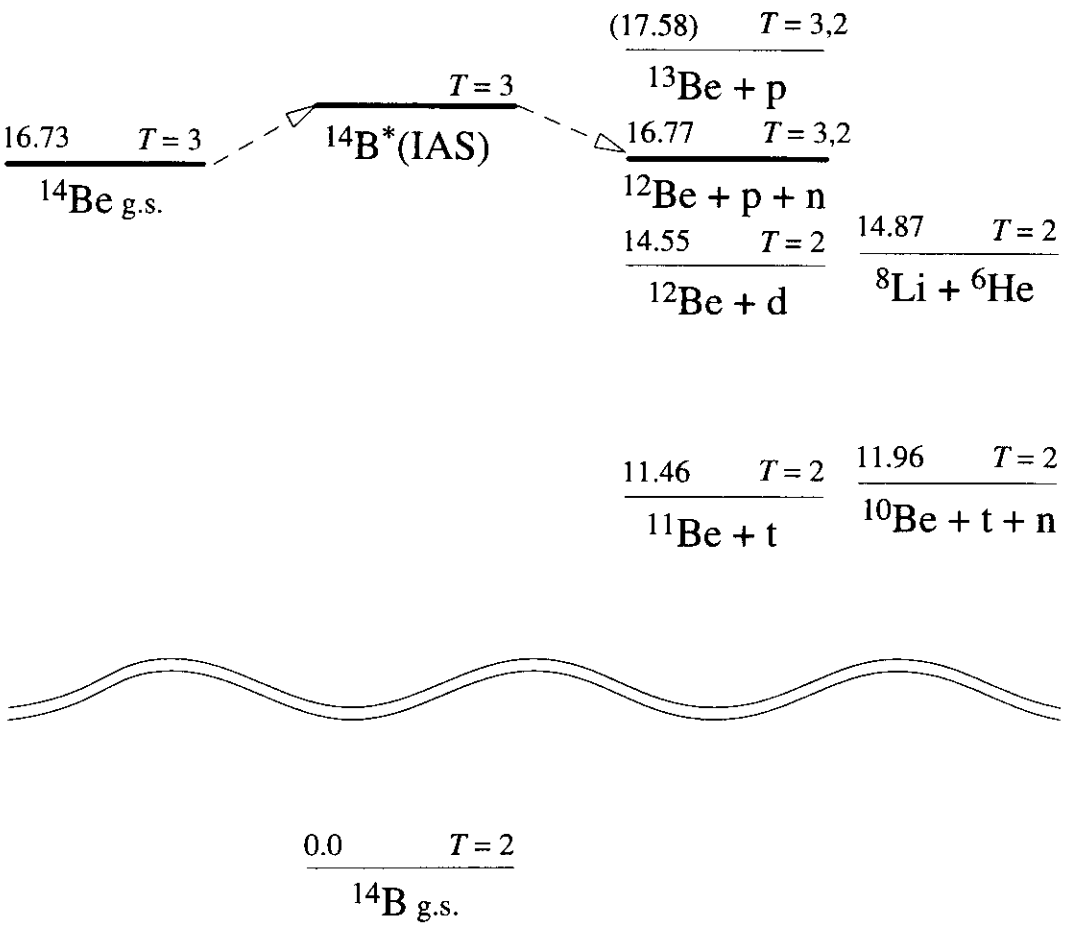

Fig. 1. Energy level scheme associated with the charge-exchange reaction ^{14}Be(p,n)^{14}B* and particle decay of ^{14}B*. Energies relative to the ^{14}B ground state are shown in MeV [7]. A mass excess, M.E. = 33.95(9) MeV is used for ^{13}Be$_{g.s.}$ reported by Belozyorov *et al.* [8]. Note that all the other channels below 11.4 MeV such as ^{13}B+n also have isospins of $T = 2$ (not shown).

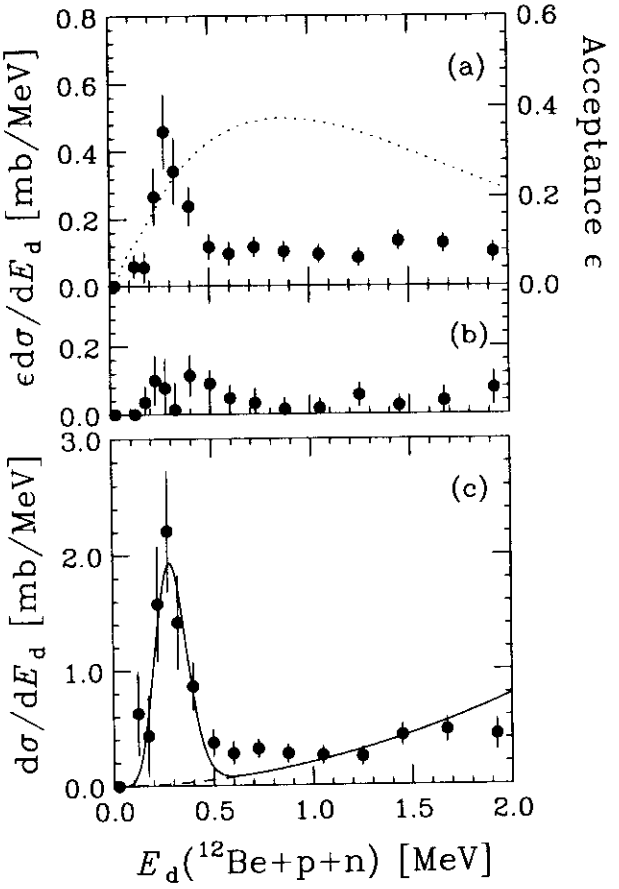

Fig. 2. Decay energy spectra of the ^{12}Be+p+n channel for (a) the (p,n) reaction and (b) the (d,2n) reaction. The dotted curve represents the detector acceptance ϵ calculated by a Monte Carlo simulation. (c) Decay energy spectrum of the same channel for the (p,n) reaction corrected by detector acceptance ϵ. The solid curve shows the fitting result with a Gaussian function and a small background with a shape of a 3-body phase space (the dashed curve).

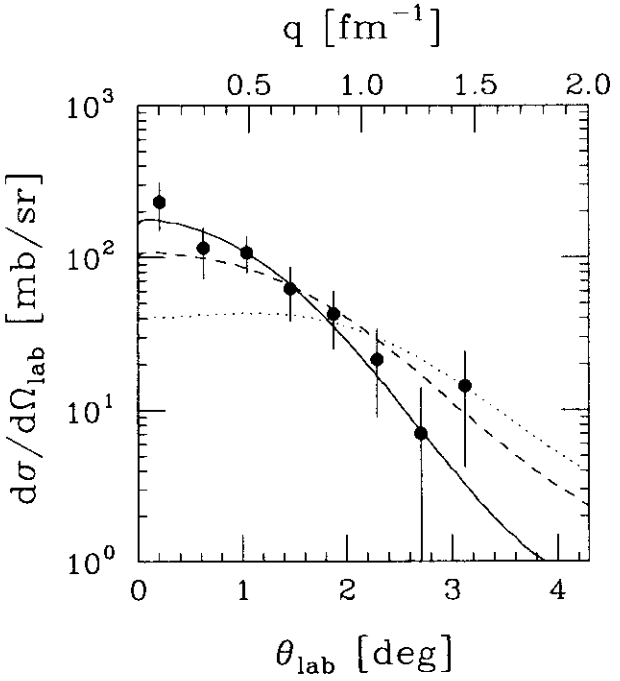

Fig. 3. Angular distribution of ^{14}B* for the $\Delta S = 0$ peak in the laboratory frame. Linear momentum transfer q is indicated as a reference. The solid, dashed and dotted curves show the results of the fitting with the spherical Bessel functions $j_\ell(qR)$ for $\ell = 0$, 1 and 2 folded with the experimental resolution, respectively.

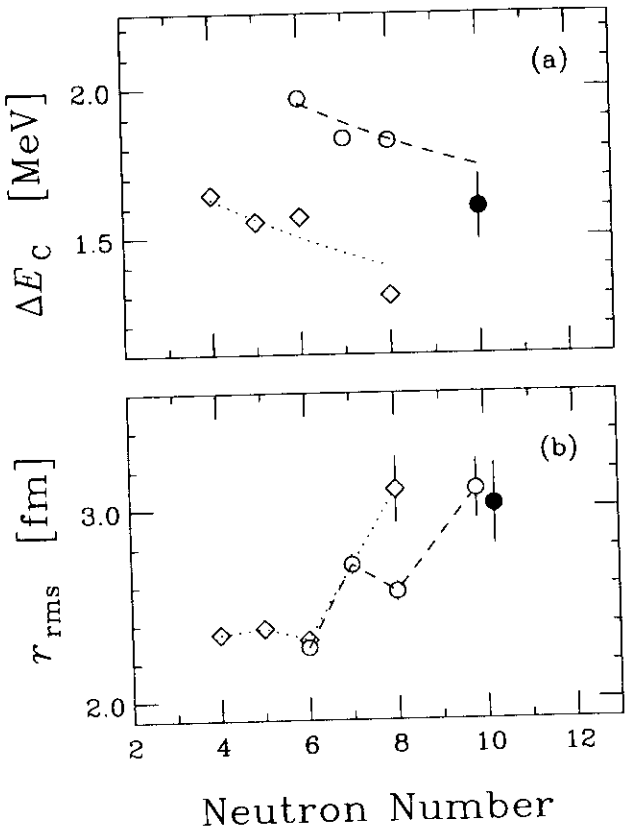

Fig. 4. (a) Coulomb displacement energy (ΔE_C) and (b) root-mean-square radii. The circles and diamonds represent Be and Li isotopes, respectively. The filled circles in both figures show the results of the present experiment. The dashed and dotted curves in the figure (a) show the calculation with a liquid-drop model using a radius parameter of $r_0 = 1.51$ fm for Li and Be isotopes, respectively. Each line in (b) is just connecting the data points for each isotope.